

# One-loop amplitudes for $W + 3$ jet production in hadron collisions

---

**R. Keith Ellis and W. T. Giele**

*Fermilab, Batavia, IL 60510, USA*

**Zoltan Kunszt**

*Institute for Theoretical Physics, ETH, CH-8093 Zürich, Switzerland*

**Kirill Melnikov**

*Department of Physics and Astronomy, Johns Hopkins University, Baltimore, MD 21218, USA*

**Giulia Zanderighi**

*Rudolf Peierls Centre for Theoretical Physics, 1 Keble Road, University of Oxford, UK*

**ABSTRACT:** We employ the recently developed method of generalized  $D$ -dimensional unitarity to compute one-loop virtual corrections to all scattering amplitudes relevant for the production of a  $W$  boson in association with three jets in hadronic collisions, treating all quarks as massless.

---

## Contents

<b>1. Introduction</b>	<b>1</b>
<b>2. The method</b>	<b>3</b>
<b>3. Dirac algebra, spinors and polarization vectors for gauge bosons</b>	<b>5</b>
3.1 Four-dimensional case	5
3.2 $D$ -dimensional case	5
<b>4. Processes with two quarks, a <math>W</math> boson and gluons</b>	<b>7</b>
4.1 Color decomposition of the amplitude	7
4.2 Numerical results for $0 \rightarrow \bar{q}qgggW$	8
<b>5. Processes with two quark pairs, a <math>W</math> boson and a gluon</b>	<b>11</b>
5.1 Color decomposition of the amplitude	11
5.2 Numerical results for $0 \rightarrow \bar{q}q\bar{Q}QgW$ amplitudes	14
<b>6. Conclusions</b>	<b>14</b>
<b>A. Numerical results</b>	<b>16</b>
A.1 Numerical results for $0 \rightarrow \bar{q}qgggW$ amplitudes	16
A.2 Numerical results for $0 \rightarrow \bar{q}q\bar{Q}QgW$ amplitudes	20

---

## 1. Introduction

Physics analyses at the LHC will benefit if accurate predictions for background and signal processes become available. Arriving at such predictions often requires next-to-leading order (NLO) QCD computations. This is particularly true for multi-particle processes where the tree-level scattering amplitudes involve the strong coupling constant at a high power. In those cases, changing the renormalization scale often leads to  $\mathcal{O}(1)$  changes in the cross-section and more accurate predictions can only be obtained with NLO computations [1].

The need for NLO corrections to processes with a vector boson and jets is particularly pressing. Corrections to vector boson + 1 jet processes and vector boson + 2 jet processes have been presented in refs. [2, 3, 4, 5] and have been successfully compared with data in refs. [6, 7]. The processes  $PP \rightarrow W/Z + N$  jets for  $N \geq 3$  have a special importance. They constitute the principal background to a number of processes, such as top-pair production and  $t$ -channel single top production. In addition,  $PP \rightarrow W/Z + N$  jet production is an important source of jets + missing energy events, which is often regarded as a key channel in the search for physics beyond the Standard Model.

Techniques for NLO computations in the Standard Model in general and in QCD in particular are well developed. Traditional methods for NLO calculations are based on the observation that each Feynman diagram can be represented as a linear combination of tensor integrals. These tensor integrals can be reduced to scalar four-, three-, two- and one-point functions by exploiting Lorentz invariance; this procedure is known as the Passarino-Veltman reduction technique [8].

While recent refinements of this procedure [9, 10, 11, 12, 13, 14, 15] have transformed it into a powerful computational tool, there are two problems inherent in it. First, the number of diagrams in a particular process grows faster than  $N!$  where  $N$  is the number of external particles. While processes with five or more external particles are rare at the Tevatron, the increase in energy and luminosity of the LHC makes consideration of processes with  $N > 5$  particles phenomenologically mandatory. Second, in the course of the Passarino-Veltman reduction procedure for high-point functions, there are numerical instabilities related to the appearance of Gram determinants. The severity of this problem also increases with the number of external particles, because of the concomitant increase in the rank of the integrals. These two problems make the application of the Passarino-Veltman reduction technique to processes with more than five external particles highly non-trivial [16, 17, 18]. For example, currently there is not a single full process with six external particles for which NLO QCD corrections are known.

While it may happen that traditional methods of one loop computations are able to overcome these problems [19, 13], it is important to develop alternative solutions. One promising approach is the method of generalized unitarity that has been developed by Bern, Dixon, Dunbar and Kosower [20]. Advances by Britto, Cachazo, Feng [21, 22] allowed the development of analytic methods for the calculation of the full amplitude, including the rational part, using recursion relations [23, 24, 25]. A further recent advance by Ossola, Pittau and Papadopoulos [26] energized attempts to develop numerical procedures based on unitarity [27, 28, 29].

A new computational scheme based on  $D$ -dimensional unitarity has been developed in Ref. [30]. We will refer to this method as generalized  $D$ -dimensional unitarity. In Refs. [31, 32] the generalized  $D$ -dimensional unitarity method was further developed and was shown to be quite robust. In particular, it was explicitly demonstrated [31] that generalized  $D$ -dimensional unitarity is an algorithm of polynomial complexity where the evaluation time for one-loop pure gluonic amplitudes with  $N$  external particles scales like  $N^9$ . Moreover, it was also shown that generalized  $D$ -dimensional unitarity can be applied to processes with massive fermions [32]. The results of these studies strongly suggest that generalized  $D$ -dimensional unitarity is an efficient computational algorithm which is now in a position to have a phenomenological impact.

The goal of this paper is to make the first steps towards the application of generalized  $D$ -dimensional unitarity to phenomenology. We focus on the computation of virtual one-loop corrections to one of the important background processes at the Tevatron and LHC for which the one-loop corrections are still unknown – the production of the  $W$  boson in association with three jets. To this end, we have to consider one-loop corrections to the

processes

$$\begin{aligned} 0 &\rightarrow \bar{u} + d + g + g + g + W^+, \\ 0 &\rightarrow \bar{u} + d + \bar{Q} + Q + g + W^+, \end{aligned} \tag{1.1}$$

and may assume, without loss of generality, that the quark  $Q$  does not couple to the  $W$  boson. We demonstrate that straightforward application of generalized  $D$ -dimensional unitarity allows us to compute *all* matrix elements required for the description of these complicated processes<sup>1</sup>.

The paper is organized as follows. In the next Section, we summarize the salient features of generalized  $D$ -dimensional unitarity. In Section 3 we discuss the Dirac algebra and the choices of the polarization vectors in four- and higher-dimensional space-times. In Section 4 we describe the computation of all primitive amplitudes relevant for the process  $0 \rightarrow \bar{u}dgggW^+$ . In Section 5 we focus on the amplitudes with four quarks, a gluon and a  $W$  boson. We conclude in Section 6. Numerical results for a specific phase-space point are collected in Appendix A.

## 2. The method

The method of calculation that we employ in this article is generalized  $D$ -dimensional unitarity. The method relies on the observation [30] that one-loop scattering amplitudes in QCD can be fully reconstructed once tree-level scattering amplitudes are known for complex on-shell momenta of external particles, in, say, six- and eight-dimensions. The necessity of knowing tree-level scattering amplitudes in higher-dimensional space-times stems from the fact that in QCD one-loop amplitudes are divergent and require regularization. Such regularization is conveniently done by continuing the dimensionality of space-time from four to  $4 - 2\epsilon$ . At the end of the calculation, the limit  $\epsilon \rightarrow 0$  is taken, but vestiges of the regularization survive as particular finite contributions (rational terms) in the scattering amplitudes. It was pointed out in [30] that the rational part of the amplitude can be determined by exploiting the dependence of residues of one-loop amplitudes on the dimensionality of space-time. Since this dependence is linear, it is sufficient to know these residues in two different space-time dimensions to reconstruct the residue as a function of  $D$ .

For technical reasons, it is convenient to deal with scattering amplitudes where external particles are ordered and no permutations are allowed. Such ordering, for example, automatically fixes the flavors of all internal lines in the highest-level  $N$ -point function that contributes to a particular  $N$ -particle ordered amplitude. It is well-known that such ordering can be achieved without sacrificing gauge-invariance [33, 34, 35]. For tree-level amplitudes, ordering of external particles appears naturally in color-ordered amplitudes. For one-loop amplitudes color ordering does not automatically lead to a complete ordering of all particles in the amplitude. To achieve this, color-ordered amplitudes are further

---

<sup>1</sup>In this article, we do not consider loop corrections with massive top quarks. Those contributions can be obtained along the lines described in [32].

decomposed into primitive amplitudes [36]. Those primitive amplitudes can be computed with the help of the color-stripped Feynman rules [36, 37, 38]. Note, however, that for a given primitive amplitude *only* color-charged particles are ordered while color-neutral particles must be inserted in all possible locations to achieve a gauge-invariant result. For our purposes, this implies that the ordering of the  $W$  boson is not fixed and we have to account for all possible insertions of the  $W$  bosons between  $\bar{u}$  and  $d$  quarks in a given primitive amplitude.

To define a primitive one-loop amplitude, we employ the following set of rules:

- we order all external particles that carry  $SU(3)$  color charge;
- we draw a parent diagram with the direction of all fermion lines fixed such that the loop is always on the right-side of an upwards oriented fermion line. The order of the external particles is defined by reading the diagram clockwise. This defines left-handed primitive amplitudes<sup>2</sup>;
- for an  $N$ -point scattering process, in general, the parent must be given by an one-particle irreducible  $N$ -point function, represented by a diagram with  $N$  propagators in the loop. For some orderings it may happen that such a parent does not exist, in this case we draw the diagram by adding dummy lines;
- we construct all possible cuts of a parent and we throw away all cuts that contain any dummy line;
- we process each cut as required by generalized  $D$ -dimensional unitarity; tree-level on-shell amplitudes, needed for the computation of residues, are calculated using color-stripped Feynman rules.

The parent primitive diagrams that are required for the calculation of  $W + 3$  jet amplitudes will be presented later in the paper.

The calculation of residues of primitive amplitudes requires the knowledge of tree-level amplitudes in six- and eight-dimensional space-time for complex momenta of external particles. The necessary matrix elements are constructed by employing Berends-Giele recurrence relations [35]. Recall, that these recurrence relations connect off-shell currents of different multiplicities and with different particle content. The on-shell scattering amplitudes are obtained from the on-shell limits of those currents. For the purposes of this paper, we need to employ currents with up to six on-shell external particles; a particular example is a fermionic current with three different fermion flavors and a gluon that contributes to some cuts of the  $\bar{u} + d + W^+ + Q + \bar{Q} + g$  scattering amplitude. We point out that, in a numerical program, it is possible to define those currents in a recursive way treating the number of external gluons as a parameter; currently, this is a necessary, (but not sufficient) prerequisite for the construction of fully automated computer codes for NLO QCD computations.

---

<sup>2</sup>There are also right-handed primitive amplitudes, where the loop is to the left of an upwards oriented fermion line. Since left and right primitive amplitudes are related, in this article we only present left primitive amplitudes [36].

### 3. Dirac algebra, spinors and polarization vectors for gauge bosons

#### 3.1 Four-dimensional case

For Dirac matrices it is convenient to use the Weyl representation where the  $\gamma$ -matrices are given by

$$\gamma^0 = \begin{pmatrix} \mathbf{0} & \mathbf{1} \\ \mathbf{1} & \mathbf{0} \end{pmatrix}, \quad \gamma^i = \begin{pmatrix} \mathbf{0} & -\sigma^i \\ \sigma^i & \mathbf{0} \end{pmatrix}, \quad \gamma^5 = \begin{pmatrix} \mathbf{1} & \mathbf{0} \\ \mathbf{0} & -\mathbf{1} \end{pmatrix}. \quad (3.1)$$

Consider a massless fermion with momentum  $p = (E, p_x, p_y, p_z)$  and let  $p_+ = E + p_z$ . Solving the Dirac equation for massless quarks, we find the following solutions

$$u_{\lambda=1}(p) = \begin{pmatrix} \sqrt{p_+} \\ (p_x + ip_y)/\sqrt{p_+} \\ 0 \\ 0 \end{pmatrix}, \quad u_{\lambda=-1}(p) = \begin{pmatrix} 0 \\ 0 \\ (p_x - ip_y)/\sqrt{p_+} \\ -\sqrt{p_+} \end{pmatrix}, \quad (3.2)$$

where  $\lambda = \pm 1$  refers to fermion helicity. Because  $p_+$  vanishes for  $E = -p_z$ , the solution for the fermion moving in the  $-z$  direction requires care. Taking the limit, we arrive at

$$u_{\lambda=1}(p) = \begin{pmatrix} 0 \\ \sqrt{2E} \\ 0 \\ 0 \end{pmatrix}, \quad u_{\lambda=-1}(p) = \begin{pmatrix} 0 \\ 0 \\ \sqrt{2E} \\ 0 \end{pmatrix}. \quad (3.3)$$

It is easy to see that in the massless case, the anti-particle solutions of the Dirac equation are related to the particle solutions so that  $v_\lambda(p) = u_{-\lambda}(p)$ .

The polarization vectors for massless gauge bosons in four dimensions are also well known. We present them here for completeness. For a gluon with momentum

$$p = E(1, \sin \theta \cos \phi, \sin \theta \sin \phi, \cos \theta),$$

the polarization vector reads

$$\epsilon_\lambda(p) = \frac{1}{\sqrt{2}} (0, \cos \theta \cos \phi - \text{sgn}(E)\lambda i \sin \phi, \cos \theta \sin \phi + \text{sgn}(E)\lambda i \cos \phi, -\sin \theta). \quad (3.4)$$

In this paper we consider outgoing gluons; for this reason, all scattering amplitudes are computed with the complex conjugate vector  $\epsilon_\lambda^*(p)$ .

#### 3.2 $D$ -dimensional case

Generalized  $D$ -dimensional unitarity requires the knowledge of tree-level scattering amplitudes in higher-dimensional space-time. To compute those amplitudes, we need  $D$ -dimensional polarization vectors for gluons, as well as spinors for fermions in  $D$  dimensions. Polarization vectors for gluons were discussed in detail in [30, 31] and we do not repeat that discussion here. Weyl fermion spinors in higher-dimensional space-time are constructed as follows.

We construct a spinor solution for a fermion with light-like momentum  $p$  by using an auxiliary light-like vector  $n$  such that  $n \cdot p \neq 0$

$$u_j(p, n) = \frac{\hat{p}}{\sqrt{2p \cdot n}} \chi_j^{(D)}(n), \quad \bar{u}_j(p, n) = \bar{\chi}_j^{(D)}(n) \frac{\hat{p}}{\sqrt{2p \cdot n}}. \quad (3.5)$$

Here  $\hat{p} = p_\mu \Gamma^\mu$ , where the summed index  $\mu$  runs over  $D$  components, (the first four of which are the  $0, x, y, z$ ) and  $\Gamma_\mu$  are the Dirac matrices in  $D$  dimensions. The index  $j$  specifies the spinor polarization states. We choose the  $D$ -dimensional,  $p$ -independent spinors  $\chi_j^{(D)}(n)$  in such a way that

$$\sum_{j=1}^{2^{(D/2-1)}} \chi_j^{(D)}(n) \otimes \bar{\chi}_j^{(D)}(n) = \hat{n}. \quad (3.6)$$

In this case, it is easy to see that the  $u_j(p, n)$  spinors satisfy both the Dirac equation for massless fermions and the completeness relation

$$\sum_{j=1}^{2^{(D/2-1)}} u_j(p, n) \otimes \bar{u}_j(p, n) = \frac{\hat{p} \hat{n} \hat{p}}{2p \cdot n} = \hat{p}. \quad (3.7)$$

We conclude that  $u_j(p, n)$  is a valid choice for on-shell fermion states.

The above construction involves an auxiliary vector  $n$  and, for this reason is quite flexible. Having such a flexibility turns out to be important, especially since we have to construct on-shell spinors for complex momenta. We give a few examples below.

We consider a  $D$ -dimensional vector  $n = (n_0, n_x, n_y, n_z, \{n_{i \in (D-4)}\})$ , choose  $n_0 = 1/2, n_z = 1/2$  and set all other components to zero. Then, we need to find the spinors  $\chi$  such that

$$\sum_{j=1}^{2^{(D/2-1)}} \chi_j^{(D)}(n) \otimes \bar{\chi}_j^{(D)}(n) = \hat{n} = \frac{1}{2} (\Gamma_0 - \Gamma_z). \quad (3.8)$$

Since  $\Gamma_{0,x,y,z}$  are all block-diagonal [39], with “blocks” being  $4 \times 4$  matrices, a  $D$ -dimensional spinor is constructed by simple iteration of the four-dimensional construction. The four-dimensional spinors are given by

$$\chi_1^{(4)} = \begin{pmatrix} 1 \\ 0 \\ 0 \\ 0 \end{pmatrix}, \quad \chi_2^{(4)} = \begin{pmatrix} 0 \\ 0 \\ 0 \\ -1 \end{pmatrix}. \quad (3.9)$$

In six dimensions the eight-component spinors are chosen to be

$$\chi_1^{(6)} = \begin{pmatrix} \chi_1^{(4)} \\ 0 \end{pmatrix}, \quad \chi_2^{(6)} = \begin{pmatrix} \chi_2^{(4)} \\ 0 \end{pmatrix}, \quad \chi_3^{(6)} = \begin{pmatrix} 0 \\ \chi_1^{(4)} \end{pmatrix}, \quad \chi_4^{(6)} = \begin{pmatrix} 0 \\ \chi_2^{(4)} \end{pmatrix}. \quad (3.10)$$

The case  $D = 8$  is a simple generalization of the above construction.

We now present two alternative procedures to define fermionic spinors which we employ when the particular choice of the vector  $n$  leads to numerical instabilities. This occurs for the on-shell momentum  $p = (p_0, 0, 0, p_0)$  since  $(p \cdot n) = 0$ . To handle this case, we change the vector  $n$  to  $n = (1/2, 0, 0, -1/2, 0_{D-4})$  in the above formulas. However, even this can be insufficient. Indeed, note that a complex momentum  $p = (0, p_x, p_y, 0)$  can be light-like. In this case, we need to choose yet another  $n$ . We can take  $n = (1, 1, 0, 0, 0_{D-4})$  and choose the following four-dimensional spinors

$$\chi_1^{(4)} = \begin{pmatrix} 1 \\ 1 \\ 0 \\ 0 \end{pmatrix}, \quad \chi_2^{(4)} = \begin{pmatrix} 0 \\ 0 \\ 1 \\ -1 \end{pmatrix}. \quad (3.11)$$

The higher-dimensional spinors are obtained from these four-dimensional solutions along the lines discussed above (see Eq.(3.10)).

#### 4. Processes with two quarks, a $W$ boson and gluons

In this section we consider the one-loop scattering amplitudes  $0 \rightarrow \bar{u} + d + (n-2)g + W^+$ . We refer to  $\bar{u}$  as  $\bar{q}$  and  $d$  as  $q$  and suppress the label of the  $W$  and its decay products in scattering amplitudes. We note that for a given primitive amplitude the  $W$  boson is inserted in all possible places when the diagram is traversed in a clockwise direction from  $\bar{q}$  to  $q$ .

##### 4.1 Color decomposition of the amplitude

At tree-level, the  $0 \rightarrow \bar{q} + q + (n-2) \text{ gluons} + W$  scattering amplitude can be written as

$$\mathcal{A}_n^{\text{tree}}(1_{\bar{q}}, 2_q, 3_g, \dots, n_g) = g^{n-2} \sum_{\sigma \in S_{n-2}} (T^{a_{\sigma(3)}} \dots T^{a_{\sigma(n)}})_{i_2}^{\bar{i}_1} A_n^{\text{tree}}(1_{\bar{q}}, 2_q; \sigma(3)_g, \dots, \sigma(n)_g), \quad (4.1)$$

where  $S_{n-2}$  is the permutation group of  $(n-2)$  elements and  $A_n^{\text{tree}}(1_{\bar{q}}, 2_q; \sigma(3)_g, \dots, \sigma(n)_g)$  are color-ordered amplitudes. For all the amplitudes computed in this paper, we take the  $W\bar{u}d$  interaction vertex to be  $-i\gamma^\mu(1 - \gamma_5)/2$ , so that neither electroweak couplings nor the Cabibbo-Kobayashi-Maskawa matrix elements are included. The  $W^+$  decays to  $\nu(q_1) + e^+(q_2)$ ; to account for this, we replace the polarization vector of the outgoing  $W$  by

$$\epsilon_\pm^\mu = (-1) \frac{\bar{u}(q_1)\gamma_\mu\gamma_\pm v(q_2)}{(q_1 + q_2)^2}, \quad \gamma_\pm = \frac{1}{2}(1 \pm \gamma_5). \quad (4.2)$$

The choice of the polarization vector  $\epsilon_-$  corresponds to the  $W$  boson interactions in the Standard Model. The generators of the  $SU(3)$  color group are normalized as  $\text{Tr}(T^a T^b) = \delta^{ab}$  and satisfy the commutation relation

$$[T^a, T^b] = -F_{ab}^c T^c. \quad (4.3)$$

This normalization allows us to employ the color-stripped Feynman rules [36, 37, 38] to calculate color-ordered scattering amplitudes.



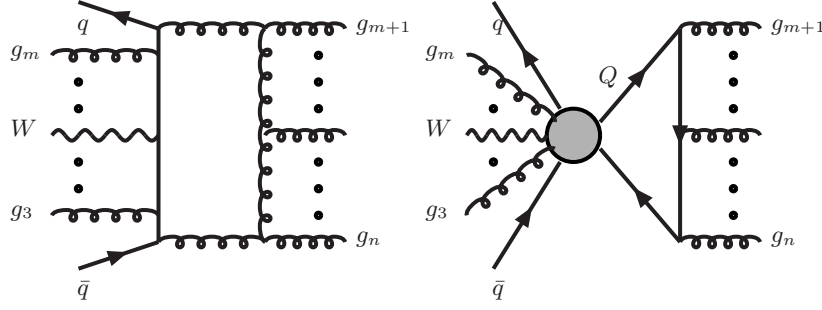


**Figure 1:** Parent diagrams for primitive amplitudes  $A_n^L(1_{\bar{q}}, 3_g, \dots, m_g, 2_q, m+1_g, \dots, n_g)$  and  $A_n^{L,[1/2]}(1_{\bar{q}}, 3_g, \dots, m_g, 2_q, (m+1)_g, \dots, n_g)$ . All other parent diagrams that contribute to this primitive are obtained by considering all possible insertions of the  $W$  boson without changing relative ordering of quarks and gluons. The shaded circle stands for dummy lines.

At one-loop, the color decomposition becomes more complicated. Using the color basis of Ref. [40], the one-loop scattering amplitude can be written as a linear combination of left primitive amplitudes

$$\begin{aligned} \mathcal{A}_n^{1\text{-loop}}(1_{\bar{q}}, 2_q, 3_g, \dots, n_g) &= g^n \left[ \sum_{p=2}^n \sum_{\sigma \in S_{n-2}} (T^{x_2} T^{a_{\sigma_3}} \dots T^{a_{\sigma_p}} T^{x_1})_{i_2}^{\bar{i}_1} (F^{a_{\sigma_{p+1}}} \dots F^{a_{\sigma_n}})_{x_1 x_2} \right. \\ &\quad \times (-1)^n A_n^L(1_{\bar{q}}, \sigma(p)_g, \dots, \sigma(3)_g, 2_q, \sigma(n)_g, \dots, \sigma(p+1)_g) \\ &\quad \left. + \frac{n_f}{N_c} \sum_{j=1}^{n-1} \sum_{\sigma \in S_{n-2}/S_{n;j}} \text{Gr}_{n;j}^{(\bar{q}q)}(\sigma_3, \dots, \sigma_n) A_{n;j}^{[1/2]}(1_{\bar{q}}, 2_q; \sigma(3)_g, \dots, \sigma(n)_g) \right], \end{aligned} \quad (4.4)$$

where for  $p=2$  the factor  $(T \dots T)_{i_2}^{\bar{i}_1} \rightarrow (T^{x_2} T^{x_1})_{i_2}^{\bar{i}_1}$  and for  $p=n$  the factor  $(F \dots F)_{x_1 x_2} \rightarrow \delta_{x_1 x_2}$ . In the second term  $S_{n;j} \equiv \mathbb{Z}_{j-1}$  is the subgroup of  $S_{n-2}$  that leaves  $\text{Gr}_{n;j}^{(\bar{q}q)}$  invariant. The color factors read

$$\begin{aligned} \text{Gr}_{n;1}^{(\bar{q}q)}(3, \dots, n) &= N_c (T^{a_3} \dots T^{a_n})_{i_2}^{\bar{i}_1}, \\ \text{Gr}_{n;2}^{(\bar{q}q)}(3; 4, \dots, n) &= 0, \\ \text{Gr}_{n;j}^{(\bar{q}q)}(3, \dots, j+1; j+2, \dots, n) &= \text{tr}(T^{a_3} \dots T^{a_{j+1}}) (T^{a_{j+2}} \dots T^{a_n})_{i_2}^{\bar{i}_1}, \quad j = 3, \dots, n-2, \\ \text{Gr}_{n;n-1}^{(\bar{q}q)}(3, \dots, n) &= \text{tr}(T^{a_3} \dots T^{a_n}) \delta_{i_2}^{\bar{i}_1}. \end{aligned} \quad (4.5)$$

Parent diagrams for primitive amplitudes that involve two quarks and gluons are shown in Fig. 1.

## 4.2 Numerical results for $0 \rightarrow \bar{q}qgggW$

We have extended the Fortran90 program Rocket [31] to include the computation of primitive amplitudes with quarks, gluons and gauge vector bosons. Rocket computes primitive amplitudes in the four-dimensional helicity scheme [41, 42]. By default, the computation is done with double precision and, if a particular phase space point is deemed numerically unstable, it is recomputed with quadruple precision using the package developed in Ref. [43]. The scalar integrals are evaluated using the QCDLoop package of ref. [44].

Note that, since Fortran90 supports recursive functions, implementation of Berends-Giele recursion for an *arbitrary* number of gluons is straightforward and indeed has been done in our program. Therefore, at least in principle, we can compute one-loop amplitudes for the process  $\bar{u}dW^+ + n$  gluons where  $n$  is an arbitrary number. We have checked that our program produces gauge-invariant one-loop amplitudes and correct  $1/\epsilon^2$  and  $1/\epsilon$  poles for  $n$  up to ten. For  $n < 3$ , we have checked that our results agree with the known one-loop amplitudes for  $W + 1$  and  $W + 2$  jets [4, 36, 45, 37]. For the description of  $W + 3$  jets, we require one-loop amplitudes with five external partons and this is what we focus on in the remainder of this paper.

We present numerical results for the primitive amplitudes with seven external particles at a particular kinematic point considered in Ref. [46]. The momenta are chosen to be

$$\begin{aligned}
p_1(\bar{q}) &= \frac{\mu}{10}(1, \cos \alpha \cos \beta, \cos \alpha \sin \beta, \sin \alpha), \\
p_2(q) &= \frac{\mu}{2}(-1, \sin \theta, \cos \theta \sin \phi, \cos \theta \cos \phi), \\
p_3(g) &= \frac{\mu}{2}(-1, -\sin \theta, -\cos \theta \sin \phi, -\cos \theta \cos \phi), \\
p_4(g) &= \frac{\mu}{3}(1, 1, 0, 0), \\
p_5(g) &= \frac{\mu}{8}(1, \cos \beta, \sin \beta, 0), \\
p_6(e^+) &= \frac{\mu}{12}(1, \cos \gamma \cos \beta, \cos \gamma \sin \beta, \sin \gamma), \\
p_7(\nu) &= -p_1 - p_2 - p_3 - p_4 - p_5 - p_6,
\end{aligned} \tag{4.6}$$

where  $\mu = 7$  GeV and

$$\theta = \frac{\pi}{4}, \quad \phi = \frac{\pi}{6}, \quad \alpha = \frac{\pi}{3}, \quad \gamma = \frac{2\pi}{3}, \quad \cos \beta = -\frac{37}{128}. \tag{4.7}$$

The momenta  $p_6$  and  $p_7$  are used to define the polarization vector of the  $W$  boson, eq.(4.2).

Our results for unrenormalized primitive amplitudes  $A_n^L$  and  $A_n^{L,[1/2]}$  are summarized in the Appendix, see Tables 1-4 and Tables 5-6, respectively. We have checked that all primitive amplitudes have correct divergences and are gauge invariant. Moreover, we have tested the validity of our results for primitive amplitudes by reproducing a diagrammatic computation of color-ordered amplitudes by taking appropriate linear combinations of primitive amplitudes. Finally, our program reproduces the results for the leading-color primitive amplitude  $A_5^L(1_{\bar{q}}, 2_q, 3_g, 4_g, 5_g)$  computed recently in Ref. [46].

Next, we address the issue of the numerical stability of the computation. As was done earlier for similar studies of gluon amplitudes, we take care of numerical instabilities by performing computations with higher precision. Since higher precision slows the computation, it is desirable to use it only for the phase-space points that suffer from numerical instabilities. The question we have to address therefore is how to detect numerical instabilities. To study this, we generate  $10^5$  random phase-space points using Rambo [47] with minimal constraints  $E_\perp > 10^{-2}\sqrt{s}$ ,  $|\eta| < 3$  and  $\Delta R = \sqrt{\Delta\eta^2 + \Delta\phi^2} > 0.4$  and calculate the primitive amplitudes for  $0 \rightarrow \bar{q}qgggW$  with double and quadruple precision. For each phase-space point, we can check whether or not the double precision computation of a

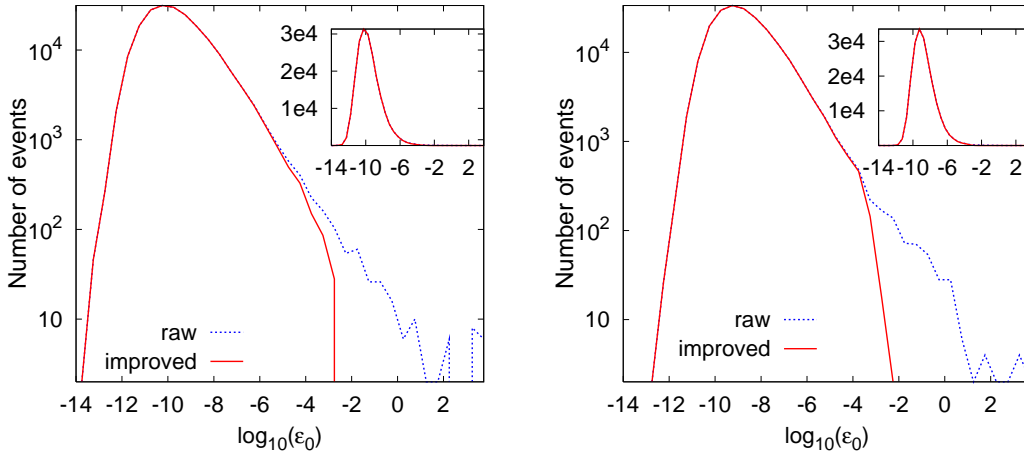


**Figure 2:** Accuracy for  $A_5^L(1_q^+, 2_q^-, 3_g^-, 4_g^+, 5_g^-)$  (left panel) and for  $A_5^L(1_q^+, 3_g^-, 4_g^+, 5_g^-, 2_q^-)$  (right panel) for  $10^5$  randomly generated phase-space points. The raw double precision data as well as the result of numerical improvements are shown (see text for details). The inset shows the same plots in a linear scale.

primitive amplitude reproduces the analytically known results for double and single poles in  $\epsilon$  and if the system of equations is solved with sufficient accuracy for each residue. To explain the latter test, we remind the reader that each residue is completely parameterized by a certain number of coefficients. We can check how well these coefficients are computed by choosing a random loop momentum, calculating the residue and checking how well this residue is obtained from the previously computed coefficients. We assign a relative error to each coefficient following the mismatch in this reconstruction. These errors are used to estimate the total error in the calculation of the primitive amplitude. By requiring that the relative precision in the poles and in the amplitude is better than  $10^{-3}$  we find that around 0.3% of the points are recomputed in quadruple precision.

After unstable points are recomputed with quadruple precision, the numerical instabilities are under control. This is demonstrated in Fig. 2 for two primitive amplitudes  $A_5^L(1_q^+, 2_q^-, 3_g^-, 4_g^+, 5_g^-)$  and  $A_5^L(1_q^+, 3_g^-, 4_g^+, 5_g^-, 2_q^-)$  where we show the number of events as a function of the relative accuracy  $\epsilon_0$  defined as the absolute value of the difference between double and quadruple precision results, divided by the quadruple precision result. We note, however, that the numerical stability of the amplitudes illustrated in Fig. 2 is generic, largely independent of the choice of the primitive amplitude and helicities of quarks and gluons. In fact, the two amplitudes considered in Fig. 2 are on the two sides of the spectrum. The leading-color amplitude  $A_5^L(1_q^+, 2_q^-, 3_g^-, 4_g^+, 5_g^-)$  has the *minimal* number of cuts, since the  $W$  boson can only be inserted in one place, between  $1_{\bar{q}}$  and  $2_q$ . On the contrary, the amplitude  $A_5^L(1_q^+, 3_g^-, 4_g^+, 5_g^-, 2_q^-)$  has the *maximal* number of cuts since the  $W$  boson can be inserted in four different places. Thus, among all primitive amplitudes with two quarks and three gluons, maximal computational effort is required for  $A_5^L(1_q^+, 3_g^-, 4_g^+, 5_g^-, 2_q^-)$  so that the issues of numerical stability may be expected to be worst in this case.

We expect that further optimization of the procedure for identifying unstable points

may be required to arrive at an optimal compromise between numerical accuracy and speed of the code. For instance, with an arbitrary precision package such as that of ref. [43], one can design a procedure where instead of using fixed quadruple precision for unstable points, the number of digits in the higher precision calculation is established according to how unstable the point is. We plan to study these issues in the future.

Finally, we remark on the CPU-time required for the evaluation of one-loop amplitudes. We find that it takes about 45-50 msec to evaluate the leading-color primitive amplitude  $A_5^L(1_{\bar{q}}, 2_q, 3_g, 4_g, 5_g)$  on a computer with 2.33 GHz Pentium Xeon processor using the intel fortran compiler. This is comparable to the evaluation times for six-gluon primitive amplitudes [31]. For more complicated primitive amplitudes, the number of cuts increases and the evaluation times scale accordingly. For example, for  $A_5^L(1_{\bar{q}}, 3_g, 4_g, 5_g, 2_q)$ , the case with the maximal number of cuts, it takes about 160 msec to compute a single primitive amplitude.

## 5. Processes with two quark pairs, a $W$ boson and a gluon

### 5.1 Color decomposition of the amplitude

We now turn to processes with two quark pairs, the  $W$  boson and a gluon,  $0 \rightarrow \bar{u} + d + \bar{Q} + Q + W + g$ . We will again refer to  $\bar{u}$  as  $\bar{q}$  and to  $d$  as  $q$ . To construct color-ordered primitive amplitudes, we assume that the  $W$  boson can not couple to the quark  $Q$ . The color decomposition of the four-quark and one-gluon amplitude at tree-level reads

$$\begin{aligned} \mathcal{B}^{\text{tree}}(1_{\bar{q}}, 2_q, 3_{\bar{Q}}, 4_Q, 5_g) = g^3 & \left[ (T^{a_5})_{i_4}^{\bar{i}_1} \delta_{i_2}^{\bar{i}_3} B_{7;1}^{\text{tree}} + \frac{1}{N_c} (T^{a_5})_{i_2}^{\bar{i}_1} \delta_{i_4}^{\bar{i}_3} B_{7;2}^{\text{tree}} \right. \\ & \left. + (T^{a_5})_{i_2}^{\bar{i}_3} \delta_{i_4}^{\bar{i}_1} B_{7;3}^{\text{tree}} + \frac{1}{N_c} (T^{a_5})_{i_4}^{\bar{i}_3} \delta_{i_2}^{\bar{i}_1} B_{7;4}^{\text{tree}} \right], \end{aligned} \quad (5.1)$$

in an obvious notation where  $a_5$  is the color index of the produced gluon. The color decomposition of the four-quark and one-gluon amplitude at one loop reads

$$\begin{aligned} \mathcal{B}^{1\text{-loop}}(1_{\bar{q}}, 2_q, 3_{\bar{Q}}, 4_Q, 5_g) = g^5 & \left[ N_c (T^{a_5})_{i_4}^{\bar{i}_1} \delta_{i_2}^{\bar{i}_3} B_{7;1} + (T^{a_5})_{i_2}^{\bar{i}_1} \delta_{i_4}^{\bar{i}_3} B_{7;2} \right. \\ & \left. + N_c (T^{a_5})_{i_2}^{\bar{i}_3} \delta_{i_4}^{\bar{i}_1} B_{7;3} + (T^{a_5})_{i_4}^{\bar{i}_3} \delta_{i_2}^{\bar{i}_1} B_{7;4} \right]. \end{aligned} \quad (5.2)$$

Each of these one-loop color-ordered amplitudes can be further written as

$$B_{7;i} = B_{7;i}^{[1]} + \frac{n_f}{N_c} B_{7;i}^{[1/2]}, \quad i = 1, 2, 3, 4, \quad (5.3)$$

to separate the diagrams with a closed fermion loop from the other ones. The amplitudes  $B_{7;i}^{[1]}$  and  $B_{7;i}^{[1/2]}$  can be written as linear combinations of primitive amplitudes. Those primitive amplitudes are shown in Figs. 3 and 4.

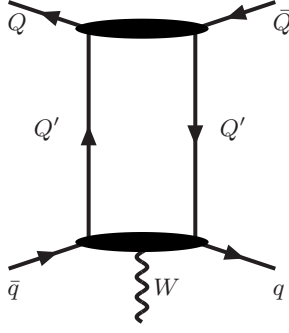


**Figure 3:** Prototype parent diagram for primitive amplitudes with four quarks, a  $W$  boson and a gluon which contain a closed fermion loop. The gluon can be inserted in four possible ways into the prototype graph, leading to four primitive amplitudes. Note that the  $W$  only couples to  $q$ . The solid blobs denote the dummy lines introduced in section 2.

For the amplitudes with an additional closed fermion loop we find

$$\begin{aligned}
B_{7;1}^{[1/2]} &= -A_L^{[1/2]}(1_{\bar{q}}, 5_g, 4_Q, 3_{\bar{Q}}, 2_q), \\
B_{7;2}^{[1/2]} &= -A_L^{[1/2]}(1_{\bar{q}}, 4_Q, 3_{\bar{Q}}, 2_q, 5_g), \\
B_{7;3}^{[1/2]} &= -A_L^{[1/2]}(1_{\bar{q}}, 4_Q, 3_{\bar{Q}}, 5_g, 2_q), \\
B_{7;4}^{[1/2]} &= -A_L^{[1/2]}(1_{\bar{q}}, 4_Q, 5_g, 3_{\bar{Q}}, 2_q).
\end{aligned} \tag{5.4}$$

The three classes of primitive amplitudes that we need to consider for four-quark processes without closed fermion loops are shown in Fig. 4,

$$B_{7;i}^{[1]} = B_{7;i}^{[1],a} + B_{7;i}^{[1],b} + B_{7;i}^{[1],c}. \tag{5.5}$$

Amplitudes from each class are written as linear combinations of primitives amplitudes.

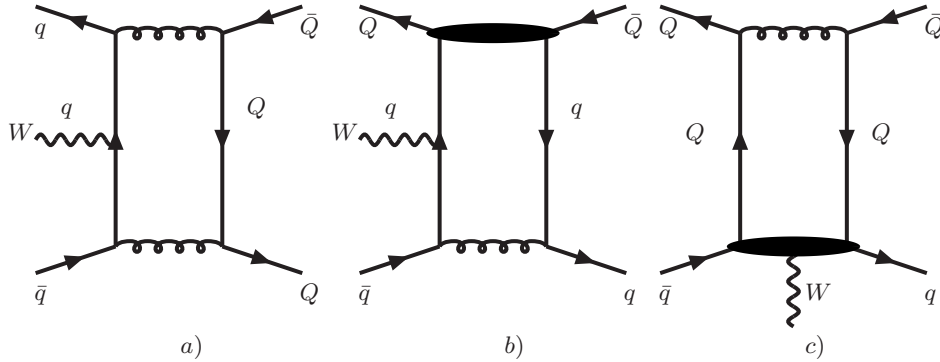


**Figure 4:** Prototype parent diagrams for primitive amplitudes with four quarks, a  $W$  boson and a gluon for classes  $a, b$  and  $c$ . The gluon can be inserted in four possible ways into any of the prototype graphs, leading to four primitive amplitudes in each case. For the diagrams in class  $b$ , all possible insertions of a  $W$  boson to a given parent primitive should be considered; note that the  $W$  only couples to  $q$ . The solid blobs denote the dummy lines introduced in section 2.

For class  $a$ , we find

$$B_{7;1}^{[1],a} = \left(1 - \frac{1}{N_c^2}\right) A_L^{[1],a}(1_{\bar{q}}, 2_q, 3_{\bar{Q}}, 4_Q, 5_g) - \frac{1}{N_c^2} \left( -A_L^{[1],a}(1_{\bar{q}}, 5_g, 2_q, 3_{\bar{Q}}, 4_Q) \right. \quad (5.6)$$

$$\left. -A_L^{[1],a}(1_{\bar{q}}, 5_g, 2_q, 4_Q, 3_{\bar{Q}}) - A_L^{[1],a}(1_{\bar{q}}, 2_q, 5_g, 3_{\bar{Q}}, 4_Q) - A_L^{[1],a}(1_{\bar{q}}, 2_q, 5_g, 4_Q, 3_{\bar{Q}}) \right. \\ \left. -A_L^{[1],a}(1_{\bar{q}}, 2_q, 3_{\bar{Q}}, 5_g, 4_Q) - A_L^{[1],a}(1_{\bar{q}}, 2_q, 4_Q, 5_g, 3_{\bar{Q}}) + A_L^{[1],a}(1_{\bar{q}}, 2_q, 4_Q, 3_{\bar{Q}}, 5_g) \right),$$

$$B_{7;2}^{[1],a} = +A_L^{[1],a}(1_{\bar{q}}, 2_q, 5_g, 4_Q, 3_{\bar{Q}}) - A_L^{[1],a}(1_{\bar{q}}, 2_q, 4_Q, 5_g, 3_{\bar{Q}}) + A_L^{[1],a}(1_{\bar{q}}, 2_q, 4_Q, 3_{\bar{Q}}, 5_g) \\ - \frac{1}{N_c^2} \left( A_L^{[1],a}(1_{\bar{q}}, 5_g, 2_q, 3_{\bar{Q}}, 4_Q) + A_L^{[1],a}(1_{\bar{q}}, 5_g, 2_q, 4_Q, 3_{\bar{Q}}) \right), \quad (5.7)$$

$$B_{7;3}^{[1],a} = \left(1 - \frac{1}{N_c^2}\right) A_L^{[1],a}(1_{\bar{q}}, 2_q, 5_g, 3_{\bar{Q}}, 4_Q) - \frac{1}{N_c^2} \left( -A_L^{[1],a}(1_{\bar{q}}, 5_g, 2_q, 3_{\bar{Q}}, 4_Q) \right. \quad (5.8)$$

$$\left. -A_L^{[1],a}(1_{\bar{q}}, 5_g, 2_q, 4_Q, 3_{\bar{Q}}) - A_L^{[1],a}(1_{\bar{q}}, 2_q, 3_{\bar{Q}}, 5_g, 4_Q) - A_L^{[1],a}(1_{\bar{q}}, 2_q, 4_Q, 5_g, 3_{\bar{Q}}) \right. \\ \left. -A_L^{[1],a}(1_{\bar{q}}, 2_q, 3_{\bar{Q}}, 4_Q, 5_g) - A_L^{[1],a}(1_{\bar{q}}, 2_q, 4_Q, 3_{\bar{Q}}, 5_g) + A_L^{[1],a}(1_{\bar{q}}, 2_q, 5_g, 4_Q, 3_{\bar{Q}}) \right),$$

$$B_{7;4}^{[1],a} = -A_L^{[1],a}(1_{\bar{q}}, 5_g, 2_q, 4_Q, 3_{\bar{Q}}) - A_L^{[1],a}(1_{\bar{q}}, 2_q, 5_g, 4_Q, 3_{\bar{Q}}) - A_L^{[1],a}(1_{\bar{q}}, 2_q, 4_Q, 3_{\bar{Q}}, 5_g) \\ - \frac{1}{N_c^2} \left( A_L^{[1],a}(1_{\bar{q}}, 2_q, 4_Q, 5_g, 3_{\bar{Q}}) + A_L^{[1],a}(1_{\bar{q}}, 2_q, 3_{\bar{Q}}, 5_g, 4_Q) \right). \quad (5.9)$$

Note that in this formula there are amplitudes where fermions and anti-fermions alternate ( $\bar{q}q\bar{Q}Q$ ) and amplitudes where this is not the case ( $\bar{q}qQ\bar{Q}$ ). The latter can be reduced to the former using the following  $C$ -parity relation

$$A_L^{[1],a}(1_{\bar{q}}, \dots, 2_q, \dots, 4_Q^{\lambda_4}, \dots, 3_{\bar{Q}}^{\lambda_3}, \dots) = (-1)^{n+1} A_L^{[1],a}(1_{\bar{q}}, \dots, 2_q, \dots, 4_{\bar{Q}}^{\lambda_4}, \dots, 3_Q^{\lambda_3}, \dots). \quad (5.10)$$

Here  $n$  is the number of *external* gluons sandwiched between the  $\bar{Q}$  and  $Q$  spinors.

For classes  $b$  and  $c$  we obtain

$$B_{7;1}^{[1],b} = \frac{1}{N_c^2} A_L^{[1],b}(1_{\bar{q}}, 5_g, 4_Q, 3_{\bar{Q}}, 2_q), \\ B_{7;2}^{[1],b} = -\frac{1}{N_c^2} \left( A_L^{[1],b}(1_{\bar{q}}, 5_g, 4_Q, 3_{\bar{Q}}, 2_q) + A_L^{[1],b}(1_{\bar{q}}, 4_Q, 5_g, 3_{\bar{Q}}, 2_q) + A_L^{[1],b}(1_{\bar{q}}, 4_Q, 3_{\bar{Q}}, 5_g, 2_q) \right), \\ B_{7;3}^{[1],b} = \frac{1}{N_c^2} A_L^{[1],b}(1_{\bar{q}}, 4_Q, 3_{\bar{Q}}, 5_g, 2_q), \\ B_{7;4}^{[1],b} = -A_L^{[1],b}(1_{\bar{q}}, 5_g, 4_Q, 3_{\bar{Q}}, 2_q) - A_L^{[1],b}(1_{\bar{q}}, 4_Q, 3_{\bar{Q}}, 5_g, 2_q) - A_L^{[1],b}(1_{\bar{q}}, 4_Q, 3_{\bar{Q}}, 2_q, 5_g) \\ - \left(1 - \frac{1}{N_c^2}\right) A_L^{[1],b}(1_{\bar{q}}, 4_Q, 5_g, 3_{\bar{Q}}, 2_q). \quad (5.11)$$

$$B_{7;1}^{[1],c} = \frac{1}{N_c^2} A_L^{[1],c}(1_{\bar{q}}, 5_g, 4_Q, 3_{\bar{Q}}, 2_q), \\ B_{7;2}^{[1],c} = -A_L^{[1],c}(1_{\bar{q}}, 5_g, 4_Q, 3_{\bar{Q}}, 2_q) - A_L^{[1],c}(1_{\bar{q}}, 4_Q, 5_g, 3_{\bar{Q}}, 2_q) - A_L^{[1],c}(1_{\bar{q}}, 4_Q, 3_{\bar{Q}}, 5_g, 2_q) \\ - \left(1 - \frac{1}{N_c^2}\right) A_L^{[1],c}(1_{\bar{q}}, 4_Q, 3_{\bar{Q}}, 2_q, 5_g),$$

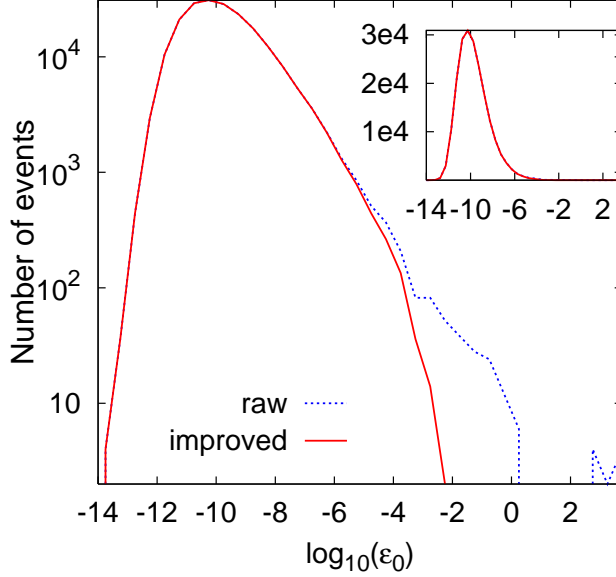


**Figure 5:** Accuracy for  $A_L^{[1],a}(1_{\bar{q}}^+, 2_q^-, 5_g^+, 3_{\bar{Q}}^-, 4_Q^+)$  amplitude for  $10^5$  randomly generated phase-space points. The raw double precision data as well as the result of numerical improvements are shown. The inset shows the same plots in a linear scale.

$$B_{7;3}^{[1],c} = \frac{1}{N_c^2} A_L^{[1],c}(1_{\bar{q}}, 4_Q, 3_{\bar{Q}}, 5_g, 2_q), \quad (5.12)$$

$$B_{7;4}^{[1],c} = -\frac{1}{N_c^2} \left( A_L^{[1],c}(1_{\bar{q}}, 5_g, 4_Q, 3_{\bar{Q}}, 2_q) + A_L^{[1],c}(1_{\bar{q}}, 4_Q, 3_{\bar{Q}}, 5_g, 2_q) + A_L^{[1],c}(1_{\bar{q}}, 4_Q, 3_{\bar{Q}}, 2_q, 5_g) \right),$$

## 5.2 Numerical results for $0 \rightarrow \bar{q}q\bar{Q}QgW$ amplitudes

We now present numerical results for  $0 \rightarrow \bar{q}q\bar{Q}QgW$  amplitudes. We use the kinematic point in Eq. (4.6), where the momentum  $p_3$  is the momentum of  $\bar{Q}$  and the momentum  $p_4$  refers to  $Q$ . The results of the calculation are given in Tables 7-11. The results for primitive amplitudes given in these Tables are sufficient to obtain numerical results for the color-ordered amplitudes  $B_{7;i}$ ,  $i = 1, \dots, 4$  using the equations given in the previous subsection. In fact, we have checked our results for the primitive amplitudes by calculating the color-ordered amplitudes  $B_{7;i}$ ,  $i = 1, \dots, 4$  diagrammatically and verifying that linear combinations of the primitive amplitudes computed with *Rocket* reproduce results of the diagrammatic computation. The numerical stability of a four-quark amplitude is illustrated in Fig. 5. It is very similar to the numerical stability of the amplitudes with two quarks and three gluons discussed earlier in detail and to other four-quark amplitudes.

## 6. Conclusions

In this paper we have shown that a straightforward application of the generalized  $D$ -dimensional unitarity method proposed in ref. [30] allows us to compute all one-loop scattering amplitudes required to describe the production of a  $W$  boson in association with

three jets at hadron colliders. We observe satisfactory performance in terms of numerical stability and required run times. We feel confident that the results of this paper provide a solid foundation for computing the one-loop virtual corrections to the production of the  $W + 3$  jets in hadron collisions.

On a more general side, the current version of `Rocket` computes one-loop amplitudes for processes  $0 \rightarrow n$  gluons,  $0 \rightarrow \bar{q}q + n$  gluons,  $0 \rightarrow \bar{q}qW + n$  gluons and  $0 \rightarrow \bar{q}q\bar{Q}QW + 1$  gluon. It is straightforward to extend the program to include similar processes with the  $Z$  boson and processes with massive quarks  $0 \rightarrow \bar{t}t + n$  gluons. This list is a testimony to the power of the method and indicates that the development of automated programs for one-loop calculations may finally be within reach.

### Acknowledgments

We acknowledge useful discussions with J.C. Winter. R.K.E and W.G are grateful to the Center for Theoretical Studies, ETH, Zürich for hospitality during the initial stage of this work. The research of K.M. is supported by the startup package provided by Johns Hopkins University. G.Z. is supported by the British Science and Technology Facilities Council. Fermilab is operated by Fermi Research Alliance, LLC under Contract No. DE-AC02-07CH11359 with the United States Department of Energy.



## A. Numerical results

In this Appendix we present the numerical results for various primitive amplitudes that we employ for the computation of  $W + 3$  jet processes. Numerical results are presented for the phase-space point given in Eq.(4.6) for various helicities of the external particles. For convenience, we present the results for the ratio of a one-loop primitive amplitude and the corresponding primitive tree-level amplitude defined as <sup>3</sup>

$$r_L^{[j]}(1, 2, 3, 4, 5, 6, 7) = \frac{1}{c_\Gamma} \frac{A_L^{[j]}(1, 2, 3, 4, 5, 6, 7)}{A^{\text{tree}}(1, 2, 3, 4, 5, 6, 7)}, \quad c_\Gamma = \frac{\Gamma(1+\epsilon)\Gamma(1-\epsilon)^2}{(4\pi)^{2-\epsilon}\Gamma(1-2\epsilon)}, \quad (\text{A.1})$$

where in this appendix we always indicate explicitly the dependence on the lepton momenta from the  $W$  decay.

### A.1 Numerical results for $0 \rightarrow \bar{q}qgggW$ amplitudes

Helicity	$1/\epsilon^2$	$1/\epsilon$	$\epsilon^0$
$A^{\text{tree}}(1_{\bar{q}}^+ 2_q^- 3_g^+ 4_g^+ 5_g^+ 6_l^+ 7_l^-)$ $r_L^{[1]}(1_{\bar{q}}^+ 2_q^- 3_g^+ 4_g^+ 5_g^+ 6_l^+ 7_l^-)$	-4.00000	-10.439578 - $i$ 9.424778	-0.006873 + $i$ 0.011728 5.993700 - $i$ 19.646278
$A^{\text{tree}}(1_{\bar{q}}^+ 2_q^- 3_g^+ 4_g^+ 5_g^- 6_l^+ 7_l^-)$ $r_L^{[1]}(1_{\bar{q}}^+ 2_q^- 3_g^+ 4_g^+ 5_g^- 6_l^+ 7_l^-)$	-4.00000	-10.439578 - $i$ 9.424778	0.010248 - $i$ 0.007726 -14.377555 - $i$ 37.219716
$A^{\text{tree}}(1_{\bar{q}}^+ 2_q^- 3_g^- 4_g^+ 5_g^+ 6_l^+ 7_l^-)$ $r_L^{[1]}(1_{\bar{q}}^+ 2_q^- 3_g^- 4_g^+ 5_g^+ 6_l^+ 7_l^-)$	-4.00000	-10.439578 - $i$ 9.424778	0.495774 - $i$ 1.274796 -1.039489 - $i$ 30.210418
$A^{\text{tree}}(1_{\bar{q}}^+ 2_q^- 3_g^- 4_g^+ 5_g^- 6_l^+ 7_l^-)$ $r_L^{[1]}(1_{\bar{q}}^+ 2_q^- 3_g^- 4_g^+ 5_g^- 6_l^+ 7_l^-)$	-4.00000	-10.439578 - $i$ 9.424778	-0.294256 - $i$ 0.223277 -1.444709 - $i$ 26.101951

**Table 1:** The primitive tree-level amplitude  $A^{\text{tree}}(1_{\bar{q}}, 2_q, 3_g, 4_g, 5_g, 6_l, 7_l)$  and the ratio  $r_L^{[1]}(1_{\bar{q}}, 2_q, 3_g, 4_g, 5_g, 6_l, 7_l)$  of a primitive one-loop amplitude to the primitive tree-level amplitudes for various helicities.

---

<sup>3</sup>Note that  $A^{\text{tree}}(1, 2, 3, 4, 5, 6, 7)$  denote here *primitive* tree-level amplitudes, as opposed to the color ordered amplitudes  $A_n^{\text{tree}}(1_{\bar{q}}, 2_q; \sigma(3)_g, \dots, \sigma(n)_g)$  appearing e.g. eq. (4.1), where the quarks are separated by a semicolon from the gluons.

Helicity	$1/\epsilon^2$	$1/\epsilon$	$\epsilon^0$
$A^{\text{tree}}(1_{\bar{q}}^+ 3_g^+ 2_q^- 4_g^+ 5_g^+ 6_{\bar{l}}^+ 7_l^-)$			$-0.005446 + i 0.009804$
$r_L^{[1]}(1_{\bar{q}}^+ 3_g^+ 2_q^- 4_g^+ 5_g^+ 6_{\bar{l}}^+ 7_l^-)$	$-3.00000$	$-8.676830 - i 6.283185$	$-1.423339 - i 14.443863$
$A^{\text{tree}}(1_{\bar{q}}^+ 3_g^+ 2_q^- 4_g^+ 5_g^- 6_{\bar{l}}^+ 7_l^-)$			$0.000364 + i 0.004550$
$r_L^{[1]}(1_{\bar{q}}^+ 3_g^+ 2_q^- 4_g^+ 5_g^- 6_{\bar{l}}^+ 7_l^-)$	$-3.00000$	$-8.676830 - i 6.283185$	$-11.406265 - i 16.485295$
$A^{\text{tree}}(1_{\bar{q}}^+ 3_g^- 2_q^- 4_g^+ 5_g^+ 6_{\bar{l}}^+ 7_l^-)$			$0.341643 - i 0.310960$
$r_L^{[1]}(1_{\bar{q}}^+ 3_g^- 2_q^- 4_g^+ 5_g^+ 6_{\bar{l}}^+ 7_l^-)$	$-3.00000$	$-8.676830 - i 6.283185$	$-5.430180 - i 21.180247$
$A^{\text{tree}}(1_{\bar{q}}^+ 3_g^- 2_q^- 4_g^+ 5_g^- 6_{\bar{l}}^+ 7_l^-)$			$0.024966 - i 0.156703$
$r_L^{[1]}(1_{\bar{q}}^+ 3_g^- 2_q^- 4_g^+ 5_g^- 6_{\bar{l}}^+ 7_l^-)$	$-3.00000$	$-8.676830 - i 6.283185$	$-4.868668 - i 21.036597$

**Table 2:** The primitive tree-level amplitude  $A^{\text{tree}}(1_{\bar{q}}, 3_g, 2_q, 4_g, 5_g, 6_{\bar{l}}, 7_l)$  and the ratio  $r_L^{[1]}(1_{\bar{q}}, 3_g, 2_q, 4_g, 5_g, 6_{\bar{l}}, 7_l)$  of a primitive one-loop amplitude to tree-level primitive amplitude for various helicities.

Helicity	$1/\epsilon^2$	$1/\epsilon$	$\epsilon^0$
$A^{\text{tree}}(1_{\bar{q}}^+ 3_g^+ 4_g^+ 2_q^- 5_g^+ 6_{\bar{l}}^+ 7_l^-)$			$-0.005563 - i 0.030746$
$r_L^{[1]}(1_{\bar{q}}^+ 3_g^+ 4_g^+ 2_q^- 5_g^+ 6_{\bar{l}}^+ 7_l^-)$	$-2.00000$	$-7.835662 - i 3.141593$	$13.662096 - i 25.637707$
$A^{\text{tree}}(1_{\bar{q}}^+ 3_g^+ 4_g^+ 2_q^- 5_g^- 6_{\bar{l}}^+ 7_l^-)$			$0.022677 + i 0.085524$
$r_L^{[1]}(1_{\bar{q}}^+ 3_g^+ 4_g^+ 2_q^- 5_g^- 6_{\bar{l}}^+ 7_l^-)$	$-2.00000$	$-7.835662 - i 3.141593$	$-9.177581 - i 16.265480$
$A^{\text{tree}}(1_{\bar{q}}^+ 3_g^- 4_g^+ 2_q^- 5_g^+ 6_{\bar{l}}^+ 7_l^-)$			$-0.098988 + i 1.958409$
$r_L^{[1]}(1_{\bar{q}}^+ 3_g^- 4_g^+ 2_q^- 5_g^+ 6_{\bar{l}}^+ 7_l^-)$	$-2.00000$	$-7.835662 - i 3.141593$	$-12.140461 - i 15.924761$
$A^{\text{tree}}(1_{\bar{q}}^+ 3_g^- 4_g^+ 2_q^- 5_g^- 6_{\bar{l}}^+ 7_l^-)$			$-0.283565 + i 0.841833$
$r_L^{[1]}(1_{\bar{q}}^+ 3_g^- 4_g^+ 2_q^- 5_g^- 6_{\bar{l}}^+ 7_l^-)$	$-2.00000$	$-7.835662 - i 3.141593$	$-13.465828 - i 13.730719$

**Table 3:** The primitive tree-level amplitude  $A^{\text{tree}}(1_{\bar{q}}, 3_g, 4_g, 2_q, 5_g, 6_{\bar{l}}, 7_l)$  and the ratio  $r_L^{[1]}(1_{\bar{q}}, 3_g, 4_g, 2_q, 5_g, 6_{\bar{l}}, 7_l)$  of a primitive one-loop amplitude to the primitive tree-level amplitude for various helicities.

Helicity	$1/\epsilon^2$	$1/\epsilon$	$\epsilon^0$
$A^{\text{tree}}(1_{\bar{q}}^+ 3_g^+ 4_g^+ 5_g^+ 2_q^- 6_{\bar{l}}^+ 7_l^-)$			$0.017883 + i 0.009214$
$r_L^{[1]}(1_{\bar{q}}^+ 3_g^+ 4_g^+ 5_g^+ 2_q^- 6_{\bar{l}}^+ 7_l^-)$	$-1.00000$	$-3.334232 - i 0.000000$	$11.973924 - i 8.033958$
$A^{\text{tree}}(1_{\bar{q}}^+ 3_g^+ 4_g^+ 5_g^- 2_q^- 6_{\bar{l}}^+ 7_l^-)$			$-0.033289 - i 0.082348$
$r_L^{[1]}(1_{\bar{q}}^+ 3_g^+ 4_g^+ 5_g^- 2_q^- 6_{\bar{l}}^+ 7_l^-)$	$-1.00000$	$-3.334232 + i 0.000000$	$-1.783190 + i 1.552944$
$A^{\text{tree}}(1_{\bar{q}}^+ 3_g^- 4_g^+ 5_g^+ 2_q^- 6_{\bar{l}}^+ 7_l^-)$			$-0.738428 - i 0.372652$
$r_L^{[1]}(1_{\bar{q}}^+ 3_g^- 4_g^+ 5_g^+ 2_q^- 6_{\bar{l}}^+ 7_l^-)$	$-1.00000$	$-3.334232 - i 0.000000$	$-5.654597 + i 0.276608$
$A^{\text{tree}}(1_{\bar{q}}^+ 3_g^- 4_g^+ 5_g^- 2_q^- 6_{\bar{l}}^+ 7_l^-)$			$0.552856 - i 0.461853$
$r_L^{[1]}(1_{\bar{q}}^+ 3_g^- 4_g^+ 5_g^- 2_q^- 6_{\bar{l}}^+ 7_l^-)$	$-1.00000$	$-3.334232 + i 0.000000$	$-6.461431 + i 1.451815$

**Table 4:** The primitive tree-level amplitude  $A^{\text{tree}}(1_{\bar{q}}, 3_g, 4_g, 5_g, 2_q, 6_{\bar{l}}, 7_l)$  and the ratio  $r_L^{[1]}(1_{\bar{q}}, 3_g, 4_g, 5_g, 2_q, 6_{\bar{l}}, 7_l)$  of a primitive one-loop amplitude to the primitive tree-level amplitude for various helicities.

Helicity	$1/\epsilon^2$	$1/\epsilon$	$\epsilon^0$
$A^{\text{tree}}(1_{\bar{q}}^+ 2_q^- 3_g^+ 4_g^+ 5_g^+ 6_{\bar{l}}^+ 7_l^-)$			$-0.006873 + i 0.011728$
$r_L^{[1/2]}(1_{\bar{q}}^+ 2_q^- 3_g^+ 4_g^+ 5_g^+ 6_{\bar{l}}^+ 7_l^-)$	$0.00000$	$0.000000 - i 0.000000$	$-6.001512 - i 26.601839$
$A^{\text{tree}}(1_{\bar{q}}^+ 2_q^- 3_g^+ 4_g^+ 5_g^- 6_{\bar{l}}^+ 7_l^-)$			$0.010248 - i 0.007726$
$r_L^{[1/2]}(1_{\bar{q}}^+ 2_q^- 3_g^+ 4_g^+ 5_g^- 6_{\bar{l}}^+ 7_l^-)$	$0.00000$	$0.000000 - i 0.000000$	$7.227836 - i 4.090839$
$A^{\text{tree}}(1_{\bar{q}}^+ 2_q^- 3_g^- 4_g^+ 5_g^+ 6_{\bar{l}}^+ 7_l^-)$			$0.495774 - i 1.274796$
$r_L^{[1/2]}(1_{\bar{q}}^+ 2_q^- 3_g^- 4_g^+ 5_g^+ 6_{\bar{l}}^+ 7_l^-)$	$0.00000$	$0.000000 + i 0.000000$	$0.096288 - i 0.114398$
$A^{\text{tree}}(1_{\bar{q}}^+ 2_q^- 3_g^- 4_g^+ 5_g^- 6_{\bar{l}}^+ 7_l^-)$			$-0.294256 - i 0.223277$
$r_L^{[1/2]}(1_{\bar{q}}^+ 2_q^- 3_g^- 4_g^+ 5_g^- 6_{\bar{l}}^+ 7_l^-)$	$0.00000$	$0.000000 + i 0.000000$	$0.164410 - i 0.134601$

**Table 5:** The primitive tree-level amplitude  $A^{\text{tree}}(1_{\bar{q}}, 2_q, 3_g, 4_g, 5_g, 6_{\bar{l}}, 7_l)$  and the ratio  $r_L^{[1/2]}(1_{\bar{q}}, 2_q, 3_g, 4_g, 5_g, 6_{\bar{l}}, 7_l)$  of a primitive one-loop amplitude to the primitive tree-level amplitude for various helicities.

Helicity	$1/\epsilon^2$	$1/\epsilon$	$\epsilon^0$
$A^{\text{tree}}(1_{\bar{q}}^+ 3_g^+ 2_q^- 4_g^+ 5_g^+ 6_{\bar{l}}^+ 7_l^-)$ $r_L^{[1/2]}(1_{\bar{q}}^+ 3_g^+ 2_q^- 4_g^+ 5_g^+ 6_{\bar{l}}^+ 7_l^-)$	0.00000	$0.000000 - i 0.000000$	$-0.005446 + i 0.009804$ $-0.127241 - i 1.316987$
$A^{\text{tree}}(1_{\bar{q}}^+ 3_g^+ 2_q^- 4_g^+ 5_g^- 6_{\bar{l}}^+ 7_l^-)$ $r_L^{[1/2]}(1_{\bar{q}}^+ 3_g^+ 2_q^- 4_g^+ 5_g^- 6_{\bar{l}}^+ 7_l^-)$	0.00000	$0.000000 + i 0.000000$	$0.000364 + i 0.004550$ $0.000000 + i 0.000000$
$A^{\text{tree}}(1_{\bar{q}}^+ 3_g^- 2_q^- 4_g^+ 5_g^+ 6_{\bar{l}}^+ 7_l^-)$ $r_L^{[1/2]}(1_{\bar{q}}^+ 3_g^- 2_q^- 4_g^+ 5_g^+ 6_{\bar{l}}^+ 7_l^-)$	0.00000	$0.000000 + i 0.000000$	$0.341643 - i 0.310960$ $-0.020783 - i 0.001593$
$A^{\text{tree}}(1_{\bar{q}}^+ 3_g^- 2_q^- 4_g^+ 5_g^- 6_{\bar{l}}^+ 7_l^-)$ $r_L^{[1/2]}(1_{\bar{q}}^+ 3_g^- 2_q^- 4_g^+ 5_g^- 6_{\bar{l}}^+ 7_l^-)$	0.00000	$0.000000 - i 0.000000$	$0.024966 - i 0.156703$ $0.000000 - i 0.000000$

**Table 6:** The primitive tree-level amplitude  $A^{\text{tree}}(1_{\bar{q}}, 3_g, 2_q, 4_g, 5_g, 6_{\bar{l}}, 7_l)$  and the ratio  $r_L^{[1/2]}(1_{\bar{q}}, 3_g, 2_q, 4_g, 5_g, 6_{\bar{l}}, 7_l)$  of the primitive one-loop amplitude to the primitive tree-level amplitude for various helicities.

## A.2 Numerical results for $0 \rightarrow \bar{q}q\bar{Q}QgW$ amplitudes

Numerical results for amplitudes with two quark pairs, a  $W$  boson and a gluon are presented in Tables below.

Helicity	$1/\epsilon^2$	$1/\epsilon$	$\epsilon^0$
$A^{\text{tree}}(1_{\bar{q}}^+ 5_g^+ 2_q^- 3_{\bar{Q}}^- 4_Q^+ 6_l^+ 7_l^-)$ $r_L^{[1],a}(1_{\bar{q}}^+ 5_g^+ 2_q^- 3_{\bar{Q}}^- 4_Q^+ 6_l^+ 7_l^-)$	-2.00000	$-1.906388 - i 6.283185$	$-1.347977 - i 0.593626$ $12.513239 - i 16.727811$
$A^{\text{tree}}(1_{\bar{q}}^+ 5_g^- 2_q^- 3_{\bar{Q}}^- 4_Q^+ 6_l^+ 7_l^-)$ $r_L^{[1],a}(1_{\bar{q}}^+ 5_g^- 2_q^- 3_{\bar{Q}}^- 4_Q^+ 6_l^+ 7_l^-)$	-2.00000	$-1.906388 - i 6.283185$	$-0.570749 - i 0.316836$ $12.452841 - i 14.482266$
$A^{\text{tree}}(1_{\bar{q}}^+ 2_q^- 5_g^+ 3_{\bar{Q}}^- 4_Q^+ 6_l^+ 7_l^-)$ $r_L^{[1],a}(1_{\bar{q}}^+ 2_q^- 5_g^+ 3_{\bar{Q}}^- 4_Q^+ 6_l^+ 7_l^-)$	-3.00000	$-6.083408 - i 3.141593$	$0.734834 - i 0.360895$ $9.466663 - i 4.461718$
$A^{\text{tree}}(1_{\bar{q}}^+ 2_q^- 5_g^- 3_{\bar{Q}}^- 4_Q^+ 6_l^+ 7_l^-)$ $r_L^{[1],a}(1_{\bar{q}}^+ 2_q^- 5_g^- 3_{\bar{Q}}^- 4_Q^+ 6_l^+ 7_l^-)$	-3.00000	$-6.083408 - i 3.141593$	$0.421057 + i 0.463392$ $7.337316 - i 3.094966$
$A^{\text{tree}}(1_{\bar{q}}^+ 2_q^- 3_{\bar{Q}}^- 5_g^+ 4_Q^+ 6_l^+ 7_l^-)$ $r_L^{[1],a}(1_{\bar{q}}^+ 2_q^- 3_{\bar{Q}}^- 5_g^+ 4_Q^+ 6_l^+ 7_l^-)$	-2.00000	$-1.906388 - i 6.283185$	$-0.288607 - i 0.043034$ $14.470591 - i 16.520704$
$A^{\text{tree}}(1_{\bar{q}}^+ 2_q^- 3_{\bar{Q}}^- 5_g^- 4_Q^+ 6_l^+ 7_l^-)$ $r_L^{[1],a}(1_{\bar{q}}^+ 2_q^- 3_{\bar{Q}}^- 5_g^- 4_Q^+ 6_l^+ 7_l^-)$	-2.00000	$-1.906388 - i 6.283185$	$-0.148841 + i 0.001847$ $10.478262 - i 16.315474$
$A^{\text{tree}}(1_{\bar{q}}^+ 2_q^- 3_{\bar{Q}}^- 4_Q^+ 5_g^+ 6_l^+ 7_l^-)$ $r_L^{[1],a}(1_{\bar{q}}^+ 2_q^- 3_{\bar{Q}}^- 4_Q^+ 5_g^+ 6_l^+ 7_l^-)$	-3.00000	$-5.946351 - i 9.424778$	$0.901749 + i 0.997556$ $10.012255 - i 29.539947$
$A^{\text{tree}}(1_{\bar{q}}^+ 2_q^- 3_{\bar{Q}}^- 4_Q^+ 5_g^- 6_l^+ 7_l^-)$ $r_L^{[1],a}(1_{\bar{q}}^+ 2_q^- 3_{\bar{Q}}^- 4_Q^+ 5_g^- 6_l^+ 7_l^-)$	-3.00000	$-5.946351 - i 9.424778$	$0.298533 - i 0.147741$ $9.462997 - i 25.465941$

**Table 7:** The primitive tree-level four-quark amplitudes  $A^{\text{tree}}$  and the ratio  $r_L^{[1],a}$  of the one-loop class  $a$  primitive amplitude to the corresponding primitive tree-level amplitude for various helicities.

Helicity	$1/\epsilon^2$	$1/\epsilon$	$\epsilon^0$
$A^{\text{tree}}(1_{\bar{q}}^+ 5_g^+ 2_q^- 4_{\bar{Q}}^+ 3_Q^- 6_l^+ 7_l^-)$ $r_L^{[1],a}(1_{\bar{q}}^+ 5_g^+ 2_q^- 4_{\bar{Q}}^+ 3_Q^- 6_l^+ 7_l^-)$	-2.00000	$-3.109446 + i 0.000000$	$-1.347977 - i 0.593626$ $7.650907 - i 1.630983$
$A^{\text{tree}}(1_{\bar{q}}^+ 5_g^- 2_q^- 4_{\bar{Q}}^+ 3_Q^- 6_l^+ 7_l^-)$ $r_L^{[1],a}(1_{\bar{q}}^+ 5_g^- 2_q^- 4_{\bar{Q}}^+ 3_Q^- 6_l^+ 7_l^-)$	-2.00000	$-3.109446 + i 0.000000$	$-0.570749 - i 0.316836$ $7.388565 + i 2.000057$
$A^{\text{tree}}(1_{\bar{q}}^+ 2_q^- 5_g^+ 4_{\bar{Q}}^+ 3_Q^- 6_l^+ 7_l^-)$ $r_L^{[1],a}(1_{\bar{q}}^+ 2_q^- 5_g^+ 4_{\bar{Q}}^+ 3_Q^- 6_l^+ 7_l^-)$	-3.00000	$-6.730261 - i 3.141593$	$0.446227 - i 0.403929$ $8.835307 - i 10.218599$
$A^{\text{tree}}(1_{\bar{q}}^+ 2_q^- 5_g^- 4_{\bar{Q}}^+ 3_Q^- 6_l^+ 7_l^-)$ $r_L^{[1],a}(1_{\bar{q}}^+ 2_q^- 5_g^- 4_{\bar{Q}}^+ 3_Q^- 6_l^+ 7_l^-)$	-3.00000	$-6.730261 - i 3.141593$	$0.272217 + i 0.464577$ $2.417473 - i 12.686072$
$A^{\text{tree}}(1_{\bar{q}}^+ 2_q^- 4_{\bar{Q}}^+ 5_g^+ 3_Q^- 6_l^+ 7_l^-)$ $r_L^{[1],a}(1_{\bar{q}}^+ 2_q^- 4_{\bar{Q}}^+ 5_g^+ 3_Q^- 6_l^+ 7_l^-)$	-2.00000	$-3.109446 + i 0.000000$	$0.288607 + i 0.043034$ $11.636607 + i 2.670357$
$A^{\text{tree}}(1_{\bar{q}}^+ 2_q^- 4_{\bar{Q}}^+ 5_g^- 3_Q^- 6_l^+ 7_l^-)$ $r_L^{[1],a}(1_{\bar{q}}^+ 2_q^- 4_{\bar{Q}}^+ 5_g^- 3_Q^- 6_l^+ 7_l^-)$	-2.00000	$-3.109446 + i 0.000000$	$0.148841 - i 0.001185$ $3.098383 - i 0.972210$
$A^{\text{tree}}(1_{\bar{q}}^+ 2_q^- 4_{\bar{Q}}^+ 3_Q^- 5_g^+ 6_l^+ 7_l^-)$ $r_L^{[1],a}(1_{\bar{q}}^+ 2_q^- 4_{\bar{Q}}^+ 3_Q^- 5_g^+ 6_l^+ 7_l^-)$	-3.00000	$-6.502556 - i 3.141593$	$0.613143 + i 0.954522$ $9.563123 - i 12.742650$
$A^{\text{tree}}(1_{\bar{q}}^+ 2_q^- 4_{\bar{Q}}^+ 3_Q^- 5_g^- 6_l^+ 7_l^-)$ $r_L^{[1],a}(1_{\bar{q}}^+ 2_q^- 4_{\bar{Q}}^+ 3_Q^- 5_g^- 6_l^+ 7_l^-)$	-3.00000	$-6.502556 - i 3.141593$	$0.149692 - i 0.146556$ $7.832425 - i 8.905177$

**Table 8:** The primitive tree-level four-quark amplitudes  $A^{\text{tree}}$  and the ratio  $r_L^{[1],a}$  of the primitive one-loop class  $a$  amplitude to the corresponding primitive tree-level amplitude for various helicities. Note the different ordering of the quarks  $Q$  and  $\bar{Q}$  compared to Table 7.

Helicity	$1/\epsilon^2$	$1/\epsilon$	$\epsilon^0$
$A^{\text{tree}}(1_{\bar{q}}^+ 5_g^+ 4_Q^+ 3_{\bar{Q}}^- 2_q^- 6_l^+ 7_l^-)$			$-0.901749 - i 0.997556$
$r_L^{[1],b}(1_{\bar{q}}^+ 5_g^+ 4_Q^+ 3_{\bar{Q}}^- 2_q^- 6_l^+ 7_l^-)$	$-1.00000$	$-3.334232 + i 0.000000$	$-8.027321 - i 0.968722$
$A^{\text{tree}}(1_{\bar{q}}^+ 5_g^- 4_Q^+ 3_{\bar{Q}}^- 2_q^- 6_l^+ 7_l^-)$			$-0.298533 + i 0.147741$
$r_L^{[1],b}(1_{\bar{q}}^+ 5_g^- 4_Q^+ 3_{\bar{Q}}^- 2_q^- 6_l^+ 7_l^-)$	$-1.00000$	$-3.334232 + i 0.000000$	$-4.397007 - i 3.109084$
$A^{\text{tree}}(1_{\bar{q}}^+ 4_Q^+ 5_g^+ 3_{\bar{Q}}^- 2_q^- 6_l^+ 7_l^-)$			$0.288607 + i 0.043034$
$r_L^{[1],b}(1_{\bar{q}}^+ 4_Q^+ 5_g^+ 3_{\bar{Q}}^- 2_q^- 6_l^+ 7_l^-)$	$-1.00000$	$-3.334232 + i 0.000000$	$-5.997531 - i 0.856042$
$A^{\text{tree}}(1_{\bar{q}}^+ 4_Q^+ 5_g^- 3_{\bar{Q}}^- 2_q^- 6_l^+ 7_l^-)$			$0.148841 - i 0.001185$
$r_L^{[1],b}(1_{\bar{q}}^+ 4_Q^+ 5_g^- 3_{\bar{Q}}^- 2_q^- 6_l^+ 7_l^-)$	$-1.00000$	$-3.334232 + i 0.000000$	$-6.462353 - i 0.674696$
$A^{\text{tree}}(1_{\bar{q}}^+ 4_Q^+ 3_{\bar{Q}}^- 5_g^+ 2_q^- 6_l^+ 7_l^-)$			$-0.734834 + i 0.360895$
$r_L^{[1],b}(1_{\bar{q}}^+ 4_Q^+ 3_{\bar{Q}}^- 5_g^+ 2_q^- 6_l^+ 7_l^-)$	$-1.00000$	$-3.334232 - i 0.000000$	$-6.039221 - i 0.200173$
$A^{\text{tree}}(1_{\bar{q}}^+ 4_Q^+ 3_{\bar{Q}}^- 5_g^- 2_q^- 6_l^+ 7_l^-)$			$-0.421057 - i 0.463392$
$r_L^{[1],b}(1_{\bar{q}}^+ 4_Q^+ 3_{\bar{Q}}^- 5_g^- 2_q^- 6_l^+ 7_l^-)$	$-1.00000$	$-3.334232 + i 0.000000$	$-6.632788 - i 0.178166$
$A^{\text{tree}}(1_{\bar{q}}^+ 3_{\bar{Q}}^- 4_Q^+ 2_q^- 5_g^+ 6_l^+ 7_l^-)$			$1.347977 + i 0.593626$
$r_L^{[1],b}(1_{\bar{q}}^+ 3_{\bar{Q}}^- 4_Q^+ 2_q^- 5_g^+ 6_l^+ 7_l^-)$	$-2.00000$	$-7.835662 - i 3.141593$	$-12.743438 - i 16.092839$
$A^{\text{tree}}(1_{\bar{q}}^+ 3_{\bar{Q}}^- 4_Q^+ 2_q^- 5_g^- 6_l^+ 7_l^-)$			$0.570749 + i 0.316836$
$r_L^{[1],b}(1_{\bar{q}}^+ 3_{\bar{Q}}^- 4_Q^+ 2_q^- 5_g^- 6_l^+ 7_l^-)$	$-2.00000$	$-7.835662 - i 3.141593$	$-14.463179 - i 14.071065$

**Table 9:** The primitive tree-level four-quark amplitudes  $A^{\text{tree}}$  and the ratio  $r_L^{[1],b}$  of the one-loop class  $b$  primitive amplitude to the corresponding primitive tree-level amplitude for various helicities.

Helicity	$1/\epsilon^2$	$1/\epsilon$	$\epsilon^0$
$A^{\text{tree}}(1_{\bar{q}}^+ 5_g^+ 4_Q^+ 3_{\bar{Q}}^- 2_q^- 6_l^+ 7_l^-)$			$-0.901749 - i 0.997556$
$r_L^{[1],c}(1_{\bar{q}}^+ 5_g^+ 4_Q^+ 3_{\bar{Q}}^- 2_q^- 6_l^+ 7_l^-)$	$-1.00000$	$-3.826559 - i 0.000000$	$-10.068901 - i 0.284089$
$A^{\text{tree}}(1_{\bar{q}}^+ 5_g^- 4_Q^+ 3_{\bar{Q}}^- 2_q^- 6_l^+ 7_l^-)$			$-0.298533 + i 0.147741$
$r_L^{[1],c}(1_{\bar{q}}^+ 5_g^- 4_Q^+ 3_{\bar{Q}}^- 2_q^- 6_l^+ 7_l^-)$	$-1.00000$	$-3.826559 - i 0.000000$	$-9.118256 - i 0.316181$
$A^{\text{tree}}(1_{\bar{q}}^+ 4_Q^+ 5_g^- 3_{\bar{Q}}^- 2_q^- 6_l^+ 7_l^-)$			$0.288607 + i 0.043034$
$r_L^{[1],c}(1_{\bar{q}}^+ 4_Q^+ 5_g^- 3_{\bar{Q}}^- 2_q^- 6_l^+ 7_l^-)$	$-2.00000$	$-5.954375 - i 3.141593$	$-6.343258 - i 9.293058$
$A^{\text{tree}}(1_{\bar{q}}^+ 4_Q^+ 5_g^- 3_{\bar{Q}}^- 2_q^+ 6_l^+ 7_l^-)$			$0.148841 - i 0.001185$
$r_L^{[1],c}(1_{\bar{q}}^+ 4_Q^+ 5_g^- 3_{\bar{Q}}^- 2_q^+ 6_l^+ 7_l^-)$	$-2.00000$	$-5.954375 - i 3.141593$	$-8.567533 - i 11.440611$
$A^{\text{tree}}(1_{\bar{q}}^+ 4_Q^+ 3_{\bar{Q}}^- 5_g^+ 2_q^- 6_l^+ 7_l^-)$			$-0.734834 + i 0.360895$
$r_L^{[1],c}(1_{\bar{q}}^+ 4_Q^+ 3_{\bar{Q}}^- 5_g^+ 2_q^- 6_l^+ 7_l^-)$	$-1.00000$	$-3.826559 + i 0.000000$	$-9.495931 + i 0.100657$
$A^{\text{tree}}(1_{\bar{q}}^+ 4_Q^+ 3_{\bar{Q}}^- 5_g^- 2_q^- 6_l^+ 7_l^-)$			$-0.421057 - i 0.463392$
$r_L^{[1],c}(1_{\bar{q}}^+ 4_Q^+ 3_{\bar{Q}}^- 5_g^- 2_q^- 6_l^+ 7_l^-)$	$-1.00000$	$-3.826559 - i 0.000000$	$-9.538700 - i 0.299195$
$A^{\text{tree}}(1_{\bar{q}}^+ 3_{\bar{Q}}^- 4_Q^+ 2_q^- 5_g^+ 6_l^+ 7_l^-)$			$1.347977 + i 0.593626$
$r_L^{[1],c}(1_{\bar{q}}^+ 3_{\bar{Q}}^- 4_Q^+ 2_q^- 5_g^+ 6_l^+ 7_l^-)$	$-1.00000$	$-3.826559 + i 0.000000$	$-9.696279 + i 0.000000$
$A^{\text{tree}}(1_{\bar{q}}^+ 3_{\bar{Q}}^- 4_Q^+ 2_q^- 5_g^- 6_l^+ 7_l^-)$			$0.570749 + i 0.316836$
$r_L^{[1],c}(1_{\bar{q}}^+ 3_{\bar{Q}}^- 4_Q^+ 2_q^- 5_g^- 6_l^+ 7_l^-)$	$-1.00000$	$-3.826559 + i 0.000000$	$-9.696279 + i 0.000000$

**Table 10:** The primitive tree-level four-quark amplitudes  $A^{\text{tree}}$  and the ratio  $r_L^{[1],c}$  of the primitive one-loop class  $c$  amplitude to the corresponding primitive tree-level amplitude for various helicities.



Helicity	$1/\epsilon^2$	$1/\epsilon$	$\epsilon^0$
$A^{\text{tree}}(1_{\bar{q}}^+ 5_g^+ 4_Q^+ 3_{\bar{Q}}^- 2_q^- 6_l^+ 7_l^-)$			$-0.901749 - i 0.997556$
$r_L^{[1/2]}(1_{\bar{q}}^+ 5_g^+ 4_Q^+ 3_{\bar{Q}}^- 2_q^- 6_l^+ 7_l^-)$	0.00000	$-0.666667 - i 0.000000$	$-2.527058 - i 0.104842$
$A^{\text{tree}}(1_{\bar{q}}^+ 5_g^- 4_Q^+ 3_{\bar{Q}}^- 2_q^- 6_l^+ 7_l^-)$			$-0.298533 + i 0.147741$
$r_L^{[1/2]}(1_{\bar{q}}^+ 5_g^- 4_Q^+ 3_{\bar{Q}}^- 2_q^- 6_l^+ 7_l^-)$	0.00000	$-0.666667 + i 0.000000$	$-2.366982 + i 0.089047$
$A^{\text{tree}}(1_{\bar{q}}^+ 4_Q^+ 5_g^+ 3_{\bar{Q}}^- 2_q^- 6_l^+ 7_l^-)$			$0.288607 + i 0.043034$
$r_L^{[1/2]}(1_{\bar{q}}^+ 4_Q^+ 5_g^+ 3_{\bar{Q}}^- 2_q^- 6_l^+ 7_l^-)$	0.00000	$-0.666666 + i 0.000000$	$-2.656572 + i 0.000000$
$A^{\text{tree}}(1_{\bar{q}}^+ 4_Q^+ 5_g^- 3_{\bar{Q}}^- 2_q^- 6_l^+ 7_l^-)$			$0.148841 - i 0.001185$
$r_L^{[1/2]}(1_{\bar{q}}^+ 4_Q^+ 5_g^- 3_{\bar{Q}}^- 2_q^- 6_l^+ 7_l^-)$	0.00000	$-0.666667 + i 0.000000$	$-2.656572 + i 0.000000$
$A^{\text{tree}}(1_{\bar{q}}^+ 4_Q^+ 3_{\bar{Q}}^- 5_g^+ 2_q^- 6_l^+ 7_l^-)$			$-0.734834 + i 0.360895$
$r_L^{[1/2]}(1_{\bar{q}}^+ 4_Q^+ 3_{\bar{Q}}^- 5_g^+ 2_q^- 6_l^+ 7_l^-)$	0.00000	$-0.666667 + i 0.000000$	$-2.887087 - i 0.164880$
$A^{\text{tree}}(1_{\bar{q}}^+ 4_Q^+ 3_{\bar{Q}}^- 5_g^- 2_q^- 6_l^+ 7_l^-)$			$-0.421057 - i 0.463392$
$r_L^{[1/2]}(1_{\bar{q}}^+ 4_Q^+ 3_{\bar{Q}}^- 5_g^- 2_q^- 6_l^+ 7_l^-)$	0.00000	$-0.666667 + i 0.000000$	$-2.749917 + i 0.137009$
$A^{\text{tree}}(1_{\bar{q}}^+ 4_Q^+ 3_{\bar{Q}}^- 2_q^- 5_g^+ 6_l^+ 7_l^-)$			$1.347977 + i 0.593626$
$r_L^{[1/2]}(1_{\bar{q}}^+ 4_Q^+ 3_{\bar{Q}}^- 2_q^- 5_g^+ 6_l^+ 7_l^-)$	0.00000	$-0.666667 + i 0.000000$	$-2.662151 + i 0.000000$
$A^{\text{tree}}(1_{\bar{q}}^+ 4_Q^+ 3_{\bar{Q}}^- 2_q^- 5_g^- 6_l^+ 7_l^-)$			$0.570749 + i 0.316836$
$r_L^{[1/2]}(1_{\bar{q}}^+ 4_Q^+ 3_{\bar{Q}}^- 2_q^- 5_g^- 6_l^+ 7_l^-)$	0.00000	$-0.666667 + i 0.000000$	$-2.662151 + i 0.000000$

**Table 11:** The primitive tree-level four-fermion amplitude  $A^{\text{tree}}$  and the ratio  $r_L^{[1/2]}$  of the primitive one-loop amplitude to primitive tree-level amplitude for various helicities.

## References

- [1] Z. Bern *et al.* [NLO Multileg Working Group], arXiv:0803.0494 [hep-ph].
- [2] R. K. Ellis, G. Martinelli and R. Petronzio, Nucl. Phys. B **211**, 106 (1983).
- [3] P. B. Arnold and M. H. Reno, Nucl. Phys. B **319**, 37 (1989) [Erratum-ibid. B **330**, 284 (1990)].
- [4] W. T. Giele, E. W. N. Glover and D. A. Kosower, Nucl. Phys. B **403** (1993) 633 [arXiv:hep-ph/9302225].
- [5] J. Campbell and R. K. Ellis, Phys. Rev. D **65**, 113007 (2002) [arXiv:hep-ph/0202176].
- [6] T. Aaltonen *et al.* [CDF Collaboration], Phys. Rev. D **77**, 011108 (2008) [arXiv:0711.4044 [hep-ex]].
- [7] T. Aaltonen *et al.* [CDF - Run II Collaboration], Phys. Rev. Lett. **100**, 102001 (2008) [arXiv:0711.3717 [hep-ex]].
- [8] G. Passarino and M. J. G. Veltman, Nucl. Phys. B **160**, 151 (1979).
- [9] A. I. Davydychev, Phys. Lett. B **263** (1991) 107.
- [10] G. Duplancic and B. Nizic, Eur. Phys. J. C **35** (2004) 105 [arXiv:hep-ph/0303184].
- [11] W. T. Giele and E. W. N. Glover, JHEP **0404** (2004) 029 [arXiv:hep-ph/0402152].
- [12] R. K. Ellis, W. T. Giele and G. Zanderighi, Phys. Rev. D **73** (2006) 014027 [arXiv:hep-ph/0508308].
- [13] A. Denner and S. Dittmaier, Nucl. Phys. B **734**, 62 (2006) [arXiv:hep-ph/0509141].
- [14] A. van Hameren, J. Vollinga and S. Weinzierl, Eur. Phys. J. C **41** (2005) 361 [arXiv:hep-ph/0502165].
- [15] T. Binoth, J. P. Guillet, G. Heinrich, E. Pilon and T. Reiter, arXiv:0810.0992 [hep-ph].
- [16] A. Denner, S. Dittmaier, M. Roth and L. H. Wieders, Phys. Lett. B **612**, 223 (2005) [arXiv:hep-ph/0502063].
- [17] R. K. Ellis, W. T. Giele and G. Zanderighi, JHEP **0605** (2006) 027 [arXiv:hep-ph/0602185].
- [18] A. Bredenstein, A. Denner, S. Dittmaier and S. Pozzorini, JHEP **0808** (2008) 108 [arXiv:0807.1248 [hep-ph]].
- [19] W. Giele, E. W. N. Glover and G. Zanderighi, Nucl. Phys. Proc. Suppl. **135** (2004) 275 [arXiv:hep-ph/0407016].
- [20] Z. Bern, L. J. Dixon, D. C. Dunbar and D. A. Kosower, Nucl. Phys. B **425**, 217 (1994) [arXiv:hep-ph/9403226].
- [21] R. Britto, F. Cachazo and B. Feng, Nucl. Phys. B **725**, 275 (2005) [arXiv:hep-th/0412103].
- [22] R. Britto, F. Cachazo and B. Feng, Nucl. Phys. B **715**, 499 (2005) [arXiv:hep-th/0412308].
- [23] Z. Bern, L. J. Dixon and D. A. Kosower, Phys. Rev. D **73** (2006) 065013 [arXiv:hep-ph/0507005].
- [24] C. F. Berger, Z. Bern, L. J. Dixon, D. Forde and D. A. Kosower, Phys. Rev. D **74** (2006) 036009 [arXiv:hep-ph/0604195].

- [25] C. F. Berger, Z. Bern, L. J. Dixon, D. Forde and D. A. Kosower, Phys. Rev. D **75** (2007) 016006 [arXiv:hep-ph/0607014].
- [26] G. Ossola, C. G. Papadopoulos and R. Pittau, Nucl. Phys. B **763**, 147 (2007) [arXiv:hep-ph/0609007].
- [27] R. K. Ellis, W. T. Giele and Z. Kunszt, JHEP **0803** (2008) 003 [arXiv:0708.2398 [hep-ph]].
- [28] G. Ossola, C. G. Papadopoulos and R. Pittau, JHEP **0803** (2008) 042 [arXiv:0711.3596 [hep-ph]].
- [29] C. F. Berger *et al.*, Phys. Rev. D **78** (2008) 036003 [arXiv:0803.4180 [hep-ph]].
- [30] W. T. Giele, Z. Kunszt and K. Melnikov, JHEP **0804**, 049 (2008) [arXiv:0801.2237 [hep-ph]].
- [31] W. T. Giele and G. Zanderighi, arXiv:0805.2152 [hep-ph].
- [32] R. K. Ellis, W. T. Giele, Z. Kunszt and K. Melnikov, arXiv:0806.3467 [hep-ph].
- [33] F. A. Berends and W. Giele, Nucl. Phys. B **294** (1987) 700.
- [34] M. L. Mangano, S. J. Parke and Z. Xu, Nucl. Phys. B **298** (1988) 653.
- [35] F.A. Berends and W. T. Giele, Nucl. Phys. B **306** (1988) 759.
- [36] Z. Bern, L. J. Dixon and D. A. Kosower, Nucl. Phys. B **437**, 259 (1995) [arXiv:hep-ph/9409393].
- [37] Z. Bern, L. J. Dixon and D. A. Kosower, Nucl. Phys. B **513**, 3 (1998) [arXiv:hep-ph/9708239].
- [38] Z. Bern, L. Dixon and D. Kosower, Ann. Rev. Nucl. Part. Sci. **46**, 109 (1996).
- [39] J. Collins, *Renormalization*, Cambridge University Press, 1984.
- [40] V. Del Duca, L. J. Dixon and F. Maltoni, Nucl. Phys. B **571**, 51 (2000) [arXiv:hep-ph/9910563].
- [41] Z. Bern and D. A. Kosower, Nucl. Phys. B **379** (1992) 451.
- [42] Z. Bern, A. De Freitas, L. J. Dixon and H. L. Wong, Phys. Rev. D **66** (2002) 085002.
- [43] David H. Bailey, A Fortran-90 Based Multiprecision System, ACM Transactions on Mathematical Software, vol. 21, no. 4, 1995, pg. 379387.
- [44] R. K. Ellis and G. Zanderighi, JHEP **0802**, 002 (2008) [arXiv:0712.1851 [hep-ph]].
- [45] J. M. Campbell, E. W. N. Glover and D. J. Miller, Phys. Lett. B **409** (1997) 503 [arXiv:hep-ph/9706297].
- [46] C. F. Berger *et al.*, arXiv:0808.0941 [hep-ph].
- [47] R. Kleiss, W. J. Stirling and S. D. Ellis, Comput. Phys. Commun. **40**, 359 (1986).